

Supplementary Information

Au nanoparticles confined in self-assembled Zn(II) metal-organic cubane cages for light-driven conversion of furfural to 2-methyl furan in biofuel production

Sahil Thakur^{a,b}, Jyoti Rohilla^a, Keshav Kumar^a, Raghbir Singh^{b}, Varinder Kaur^{a*}, Raman Kamboj^b*

^aDepartment of Chemistry, Panjab University, Sector-14, Chandigarh-160014, India

^bDepartment of Chemistry, DAV College, Sector 10, Chandigarh-160011, India

*Corresponding author: var_ka04@yahoo.co.in (V.K.), raghubirsingh@davchd.ac.in (R.S.)

List of Figures and Tables		
Figure S1	FT-IR spectrum of Zn cubane	S3
Figure S2	^1H -NMR spectrum (500 MHz, DMSO-d ₆) of Zn cubane	S4
Figure S3	ESI-MS spectrum of Zn cubane	S5
Figure S4	^1H -NMR spectrum (500 MHz, DMSO-d ₆) of ZnCC@AuNPs	S6
Figure S5	a) N ₂ adsorption-desorption of Zn(II) Cubane, b) N ₂ adsorption-desorption of ZnCC@AuNPs , c) BJH pore size distribution of Zn Cubane, and d) BJH pore size distribution of ZnCC@AuNPs	S7
Figure S6	a) Elemental mapping of all elements of the cubane cage (C, H, N, Br, and Zn) and b) Zn@Au(0)NPs (C, H, N, Br, Zn, and Au) at the surface.	S8
Figure S7	DLS particle size distribution of gold nanoparticles (AuNPs).	S9
Figure S8	Xps spectra of Zn Cubane showing presence Br 3d, N 1s, Zn 2p, C 1s, and O 1s elements.	S10
Figure S9	Xps spectra of ZnCC@AuNPs showing presence of Au(0) 4f, O 1s, Zn 2p, Br 3d, C 1s, and N 1s elements.	S11
Figure S10	a) PXRD pattern of Zn(II) Cubane showing a comparison of both experimental and simulated data, b) PXRD pattern of ZnCC@AuNPs and ZnCC@AuNPs after 5 catalytic cycles.	S12
Figure S11	a) UV absorption spectrum of Zn Cubane, b) UV absorption spectrum of ZnCC@AuNPs	S13
Figure S12	The effect of the temperature on the Furfural conversion and product selectivity.	S13
Figure S13	^1H -NMR spectrum (500 MHz, CDCl ₃) of 2-methyl furan product.	S14
Figure S14	^{13}C -NMR spectrum (125 MHz, CDCl ₃) of 2-methyl furan product.	S15
Figure S15	HPLC chromatogram of reference furfural, furan, and 2-methyl furan product.	S16
Figure S16	Time-scaled UV-visible spectra for the catalytic transformation reaction of furfural to 2-MF in the presence of ZnCC@AuNPs and NaOH at 60 °C in IPA.	S17
Figure S17	Recyclability of the ZnCC@AuNPs catalyst	S18
Table S1	Crystallographic data and structural parameters for zinc(II) cubane.	S19
Table S2	Bonding parameters for zinc(II) cubane.	S20
Table S3	Comparison of the catalytic activity of different catalysts for the conversion of furfural to 2-methyl furan	S21

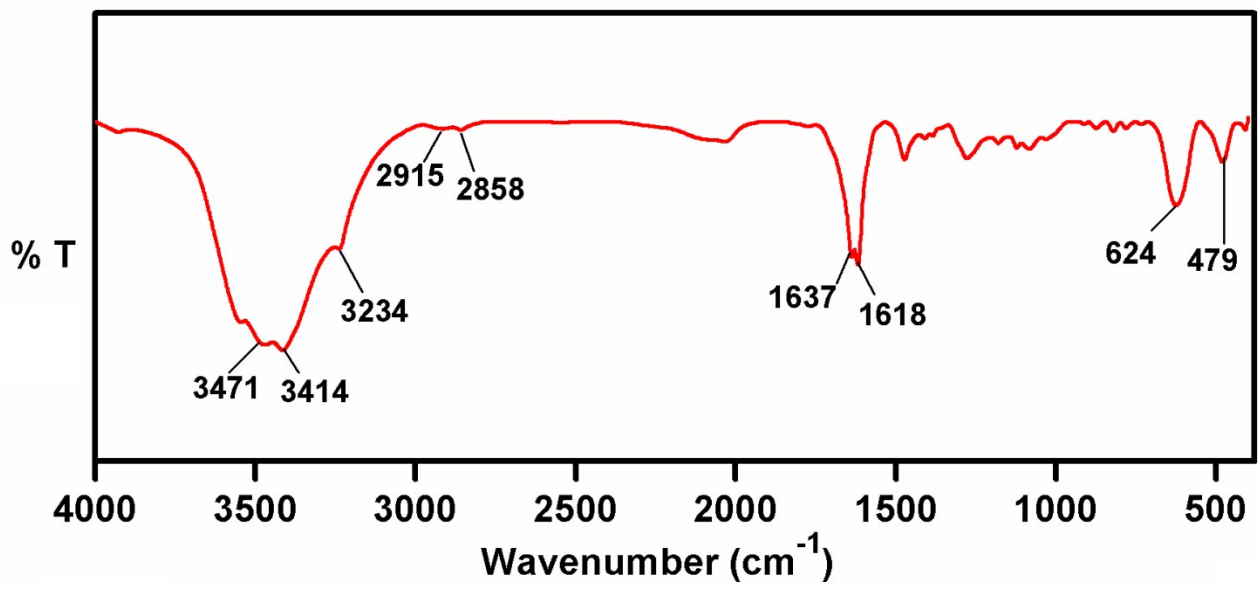


Fig. S1 FT-IR spectrum of Zn(II) cubane

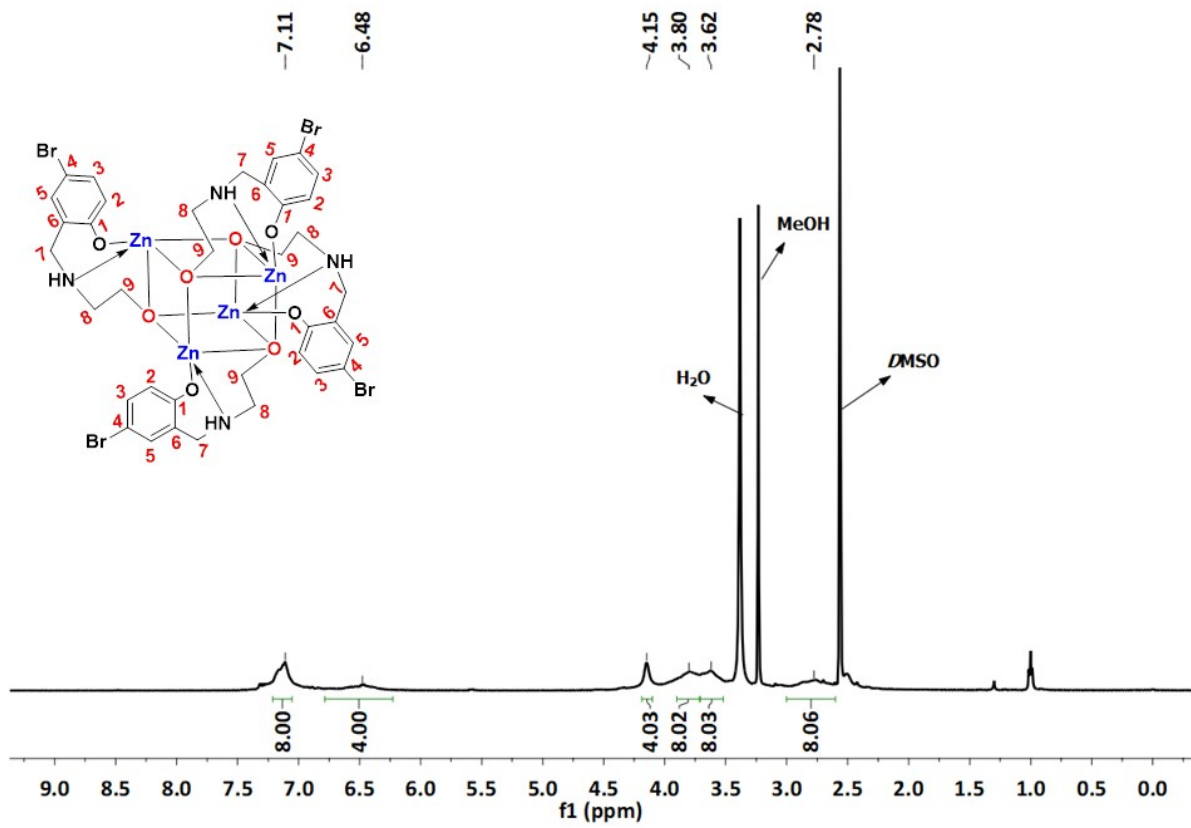


Fig. S2 ^1H -NMR spectrum (500 MHz, DMSO-d_6) of Zn(II) cubane

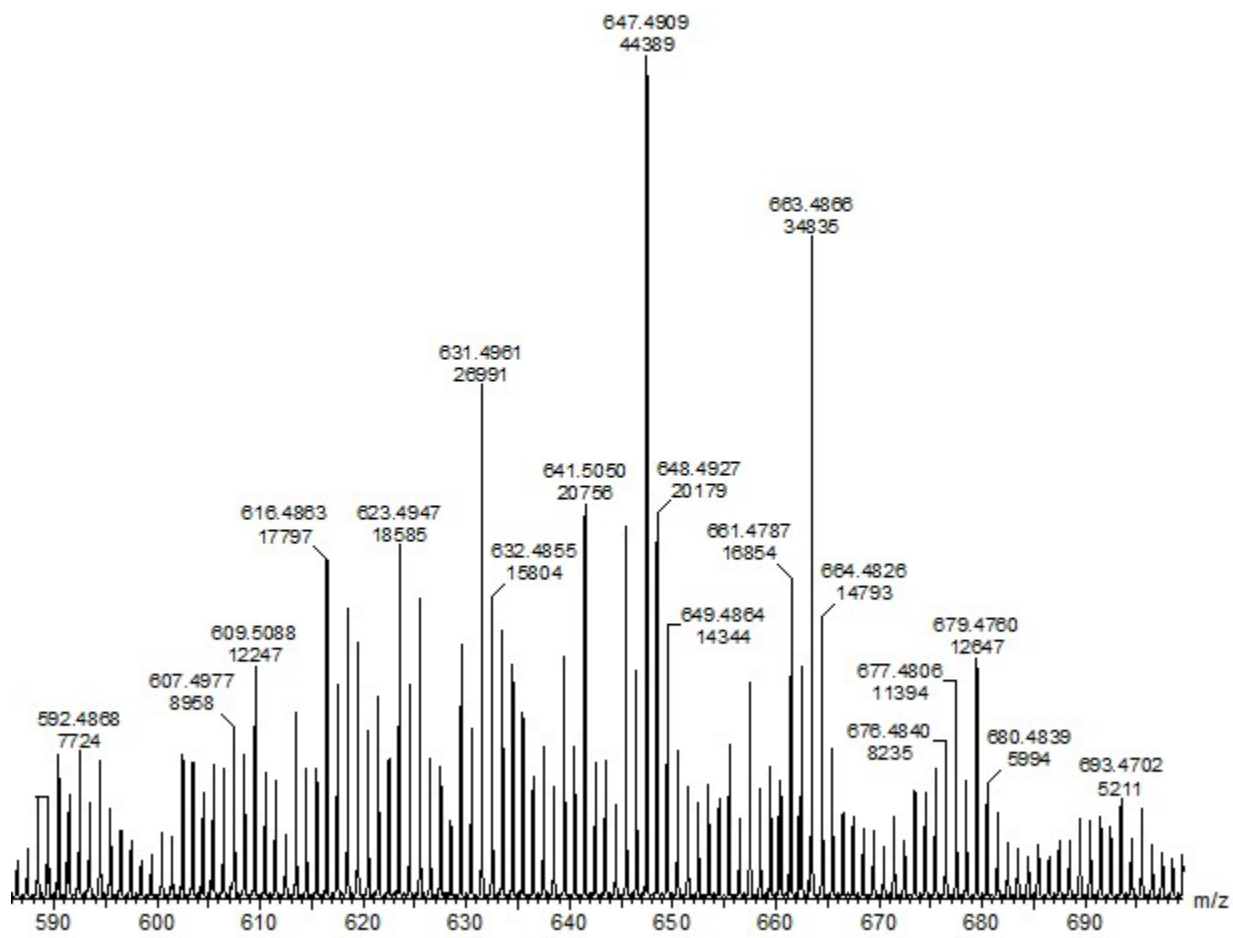


Fig. S3 ESI-MS spectrum of Zn(II) cubane $[M+H]^{2+}$ peak

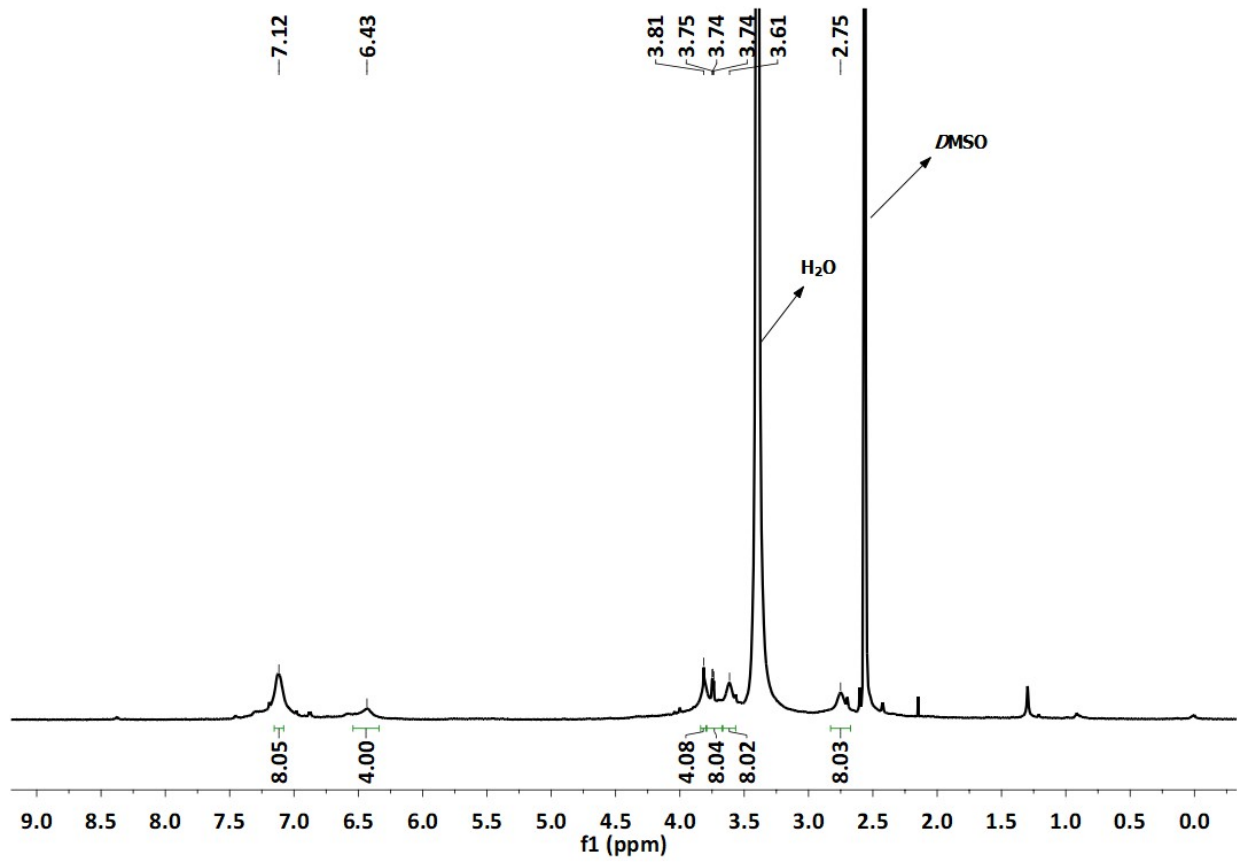


Fig. S4 ^1H -NMR spectrum (500 MHz, DMSO-d_6) of ZnCC@AuNPs

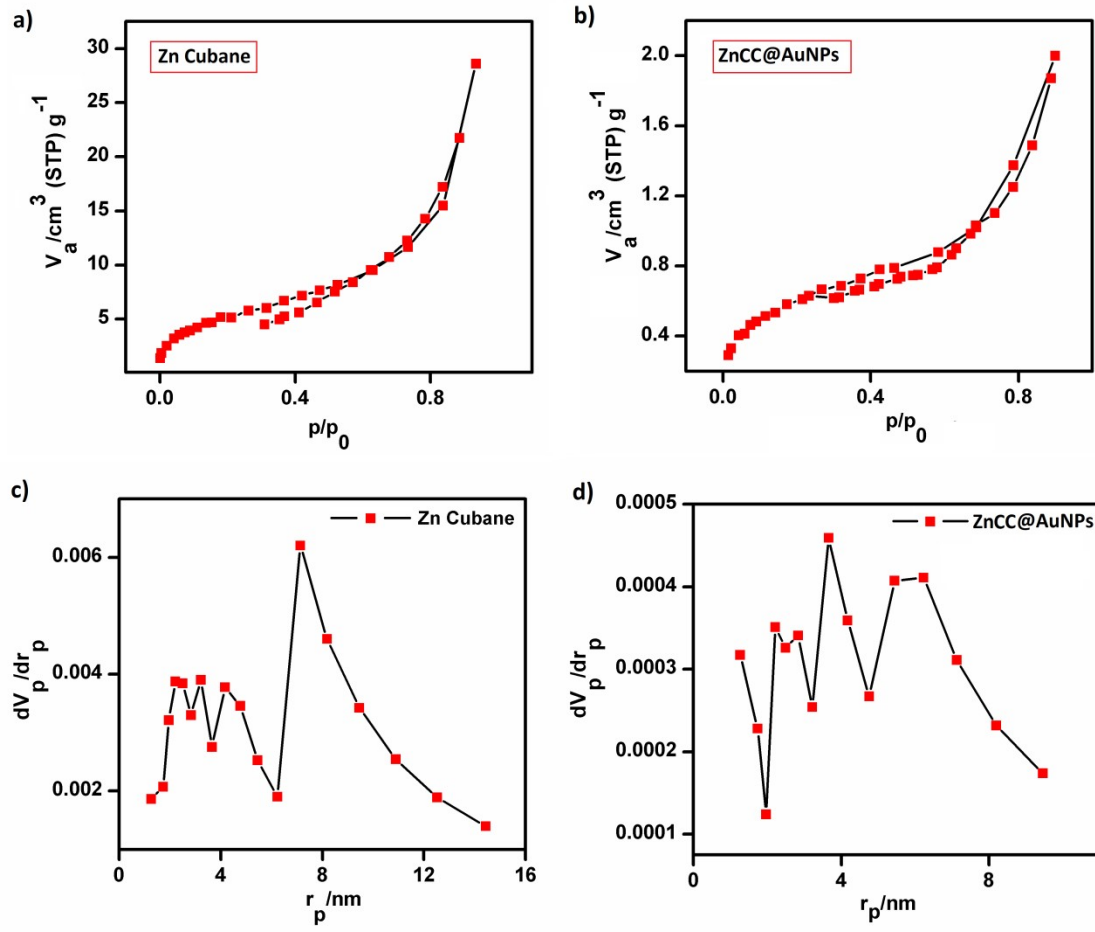
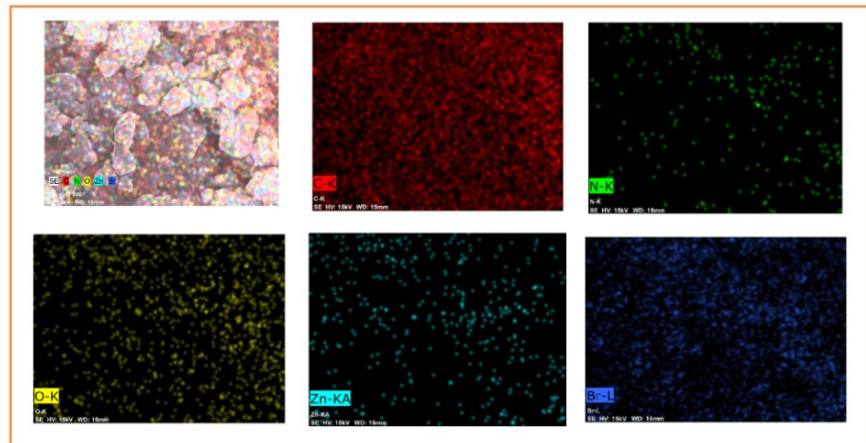


Fig. S5 a) N_2 adsorption-desorption of Zn(II) Cubane, b) N_2 adsorption-desorption of ZnCC@AuNPs, c) BJH pore size distribution of Zn Cubane, and d) BJH pore size distribution of ZnCC@AuNPs

a)



b)

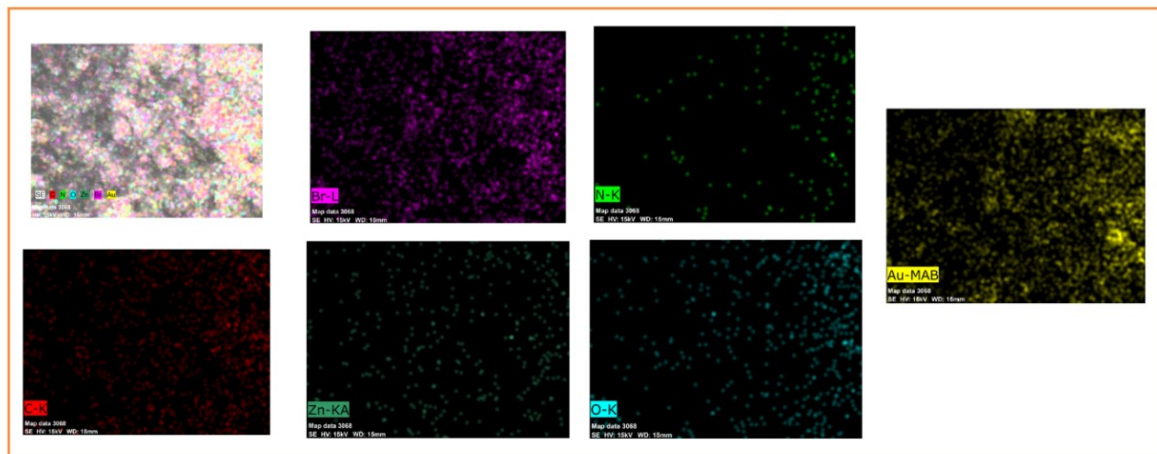


Fig. S6 a) Elemental mapping of all elements of the cubane cage (C, H, N, Br, and Zn) and b) ZnCC@AuNPs (C, H, N, Br, Zn, and Au) at the surface.

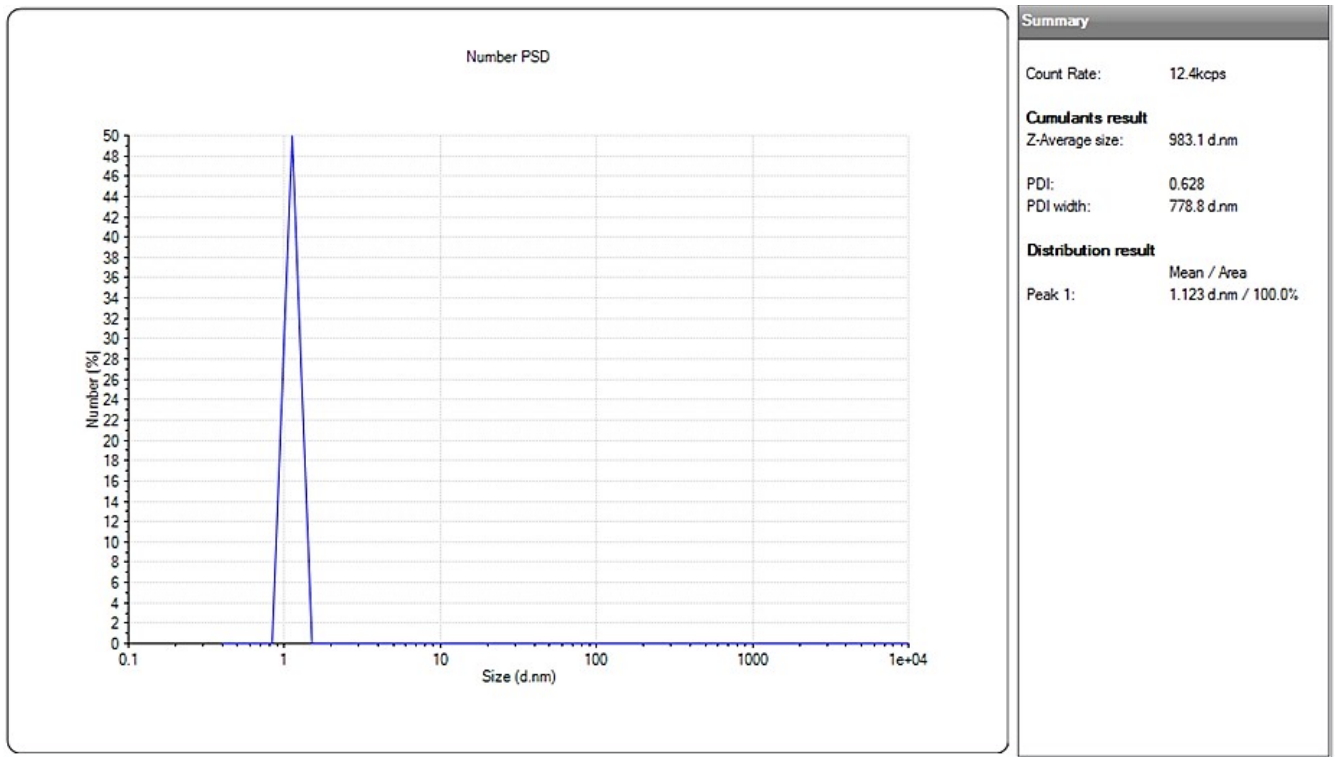


Fig. S7 DLS particle size distribution of gold nanoparticles (AuNPs).

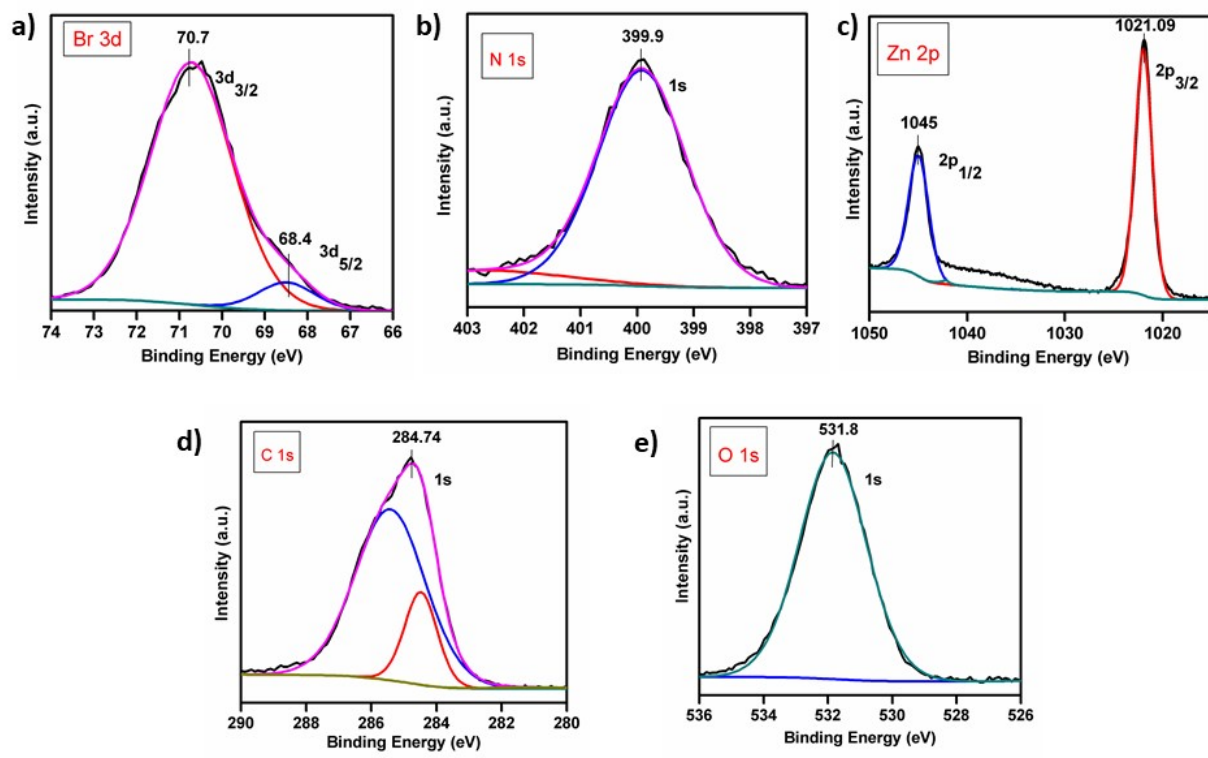


Fig. S8 Xps spectra of Zn Cubane showing the presence of Br 3d, N 1s, Zn 2p, C 1s, and O 1s elements.

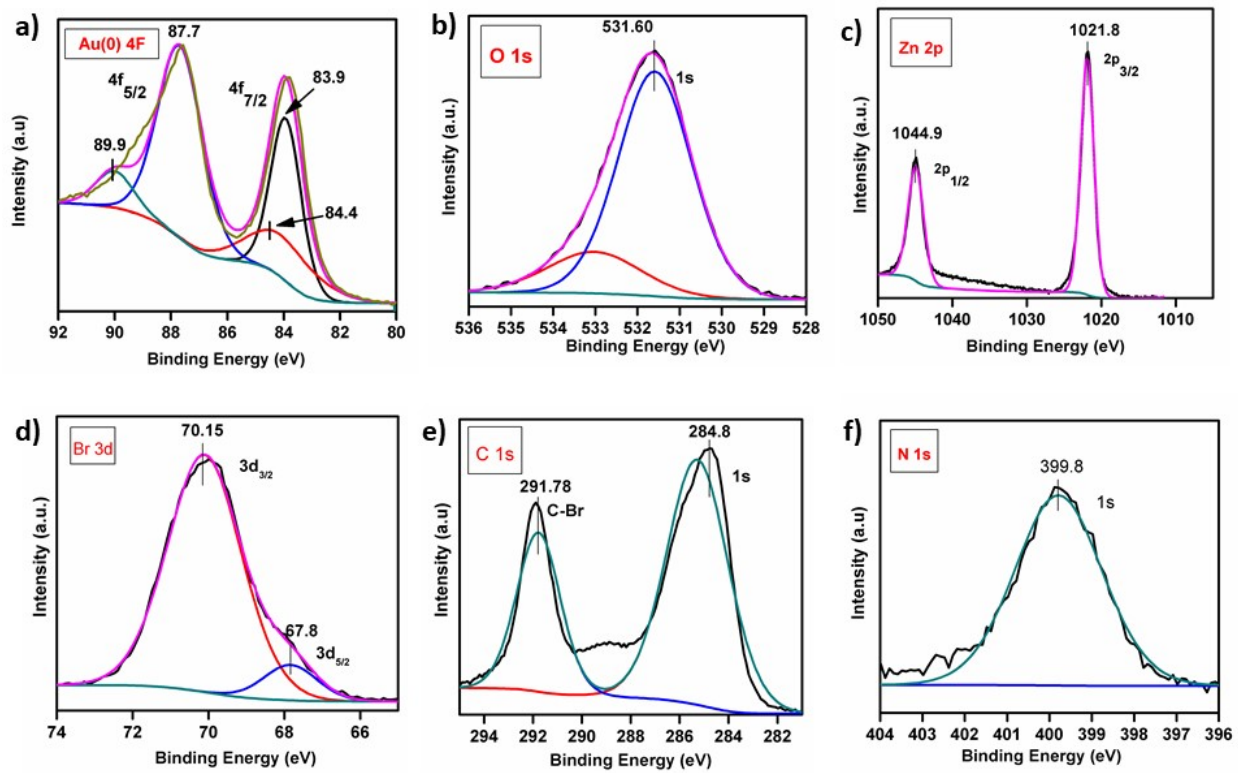


Fig. S9 Xps spectra of ZnCC@AuNPs showing presence of Au(0) 4f, O 1s, Zn 2p, Br 3d, C 1s, and N 1s elements.

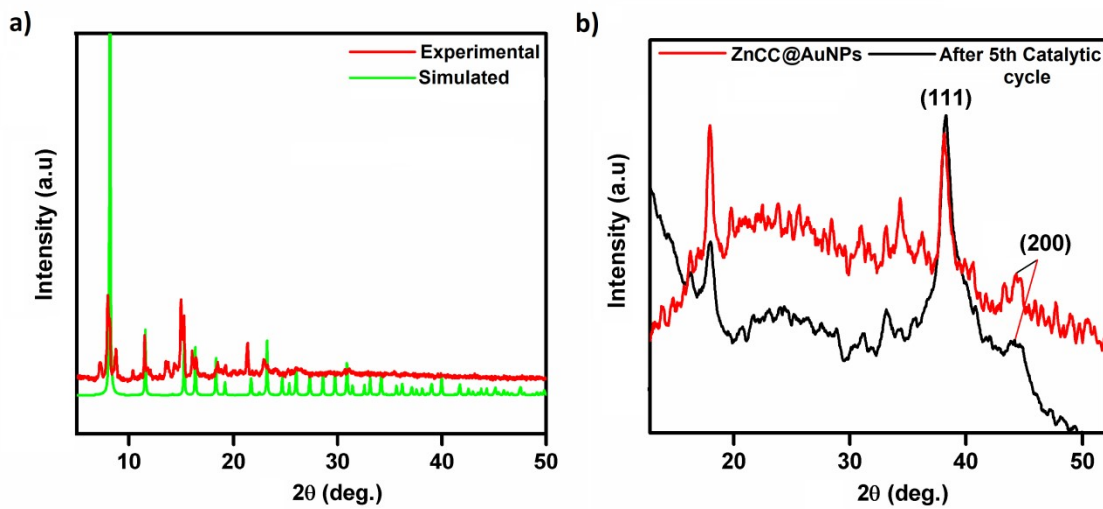


Fig. S10. a) PXRD pattern of Zn(II) Cubane showing a comparison of both experimental and simulated data, b) PXRD pattern of ZnCC@AuNPs and ZnCC@AuNPs after 5 catalytic cycles.

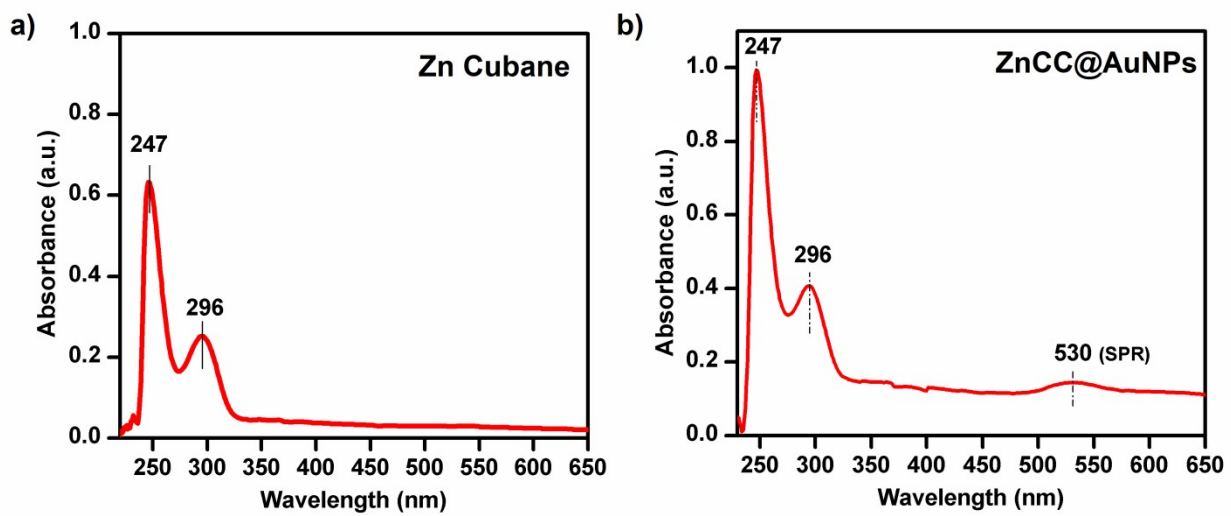


Fig. S11. a) UV absorption spectrum of Zn Cubane, b) UV absorption spectrum of ZnCC@AuNPs.

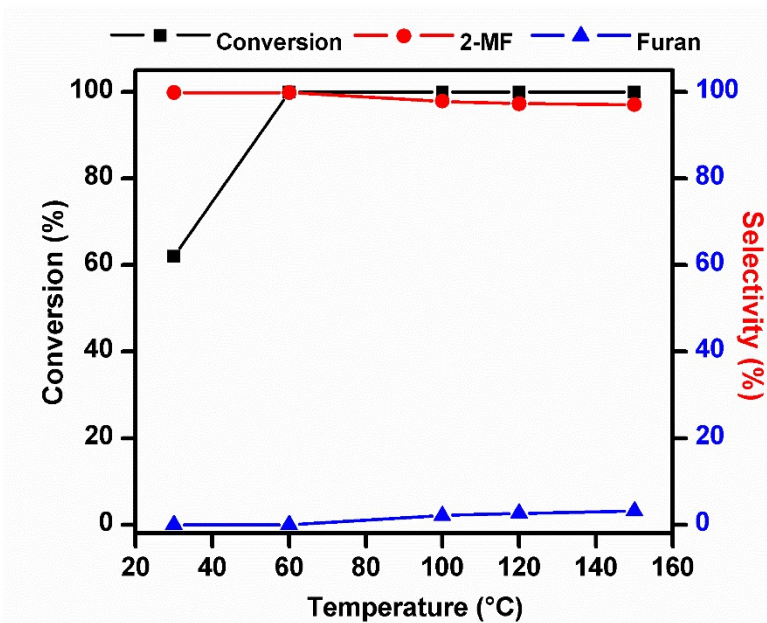


Fig. S12 The effect of the temperature on the Furfural conversion and product selectivity.

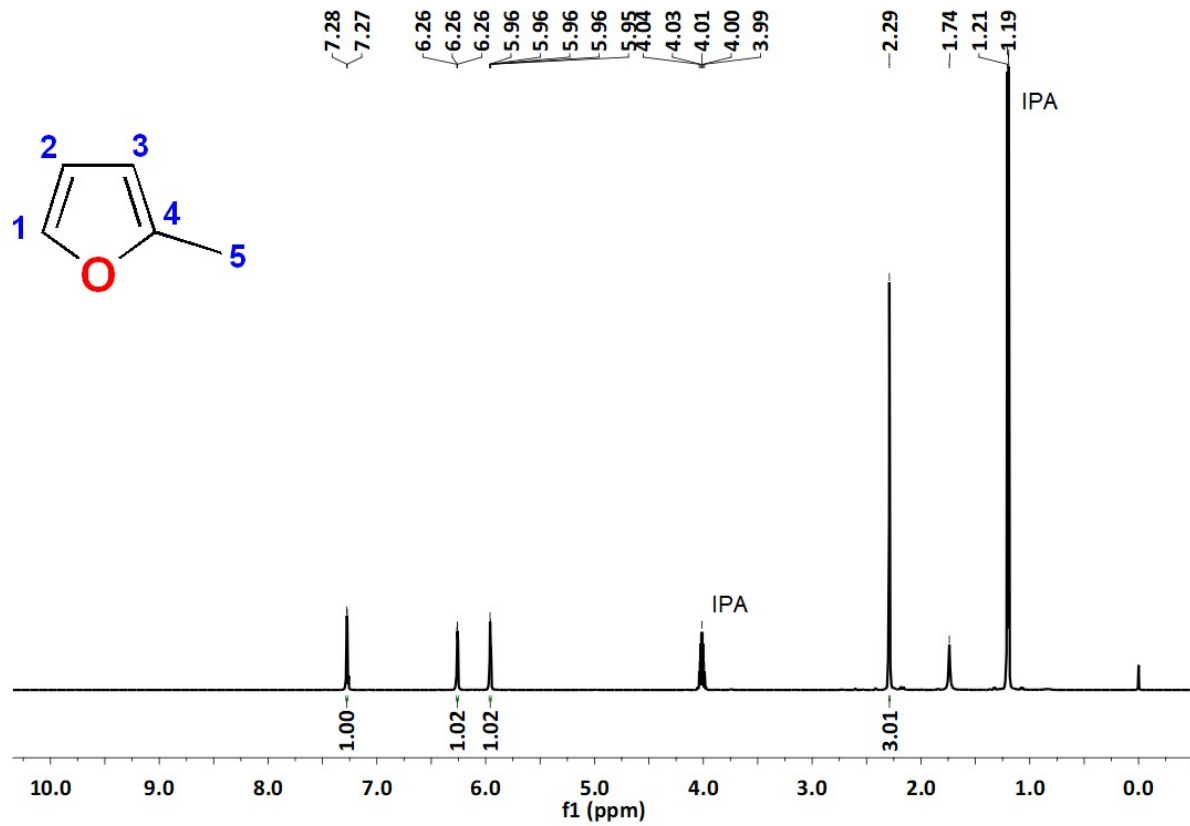


Fig. S13 ^1H -NMR spectrum (500 MHz, CDCl_3) of 2-methyl furan product.

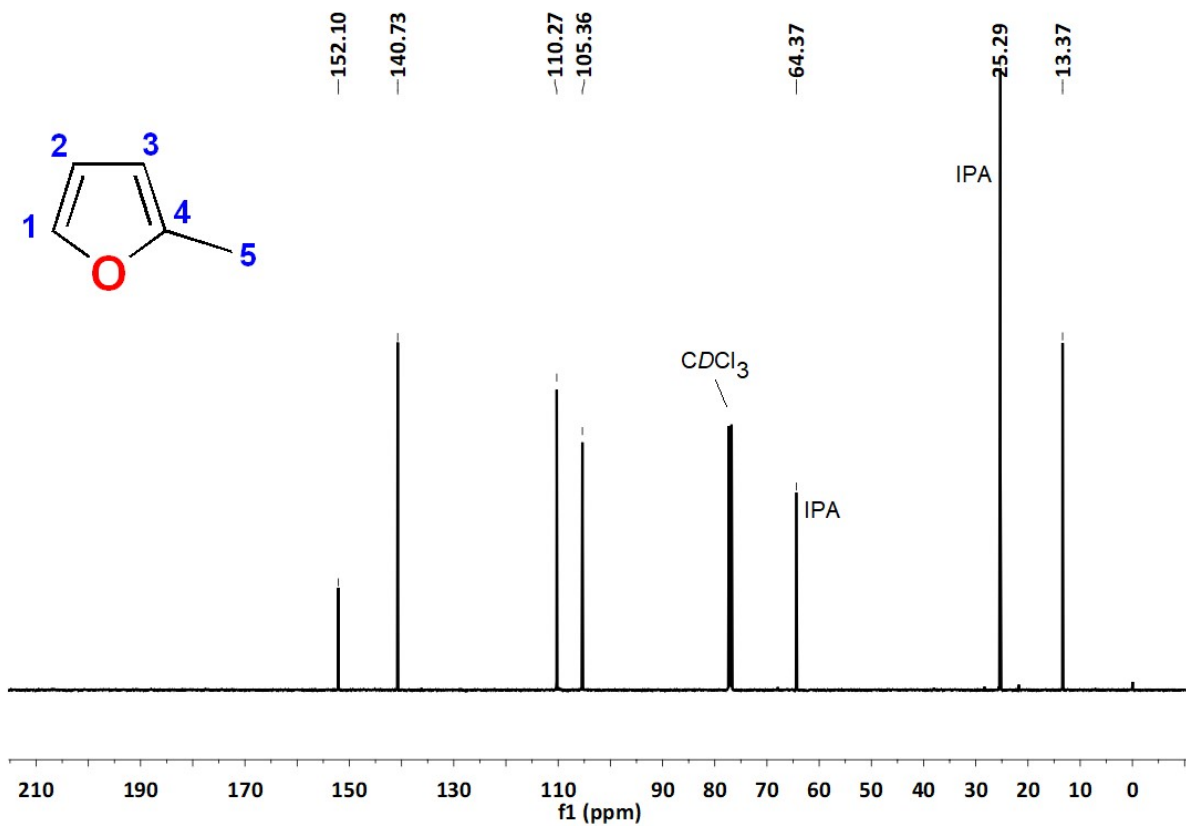


Fig. S14 ^{13}C -NMR spectrum (125 MHz, CDCl_3) of 2-methyl furan product.

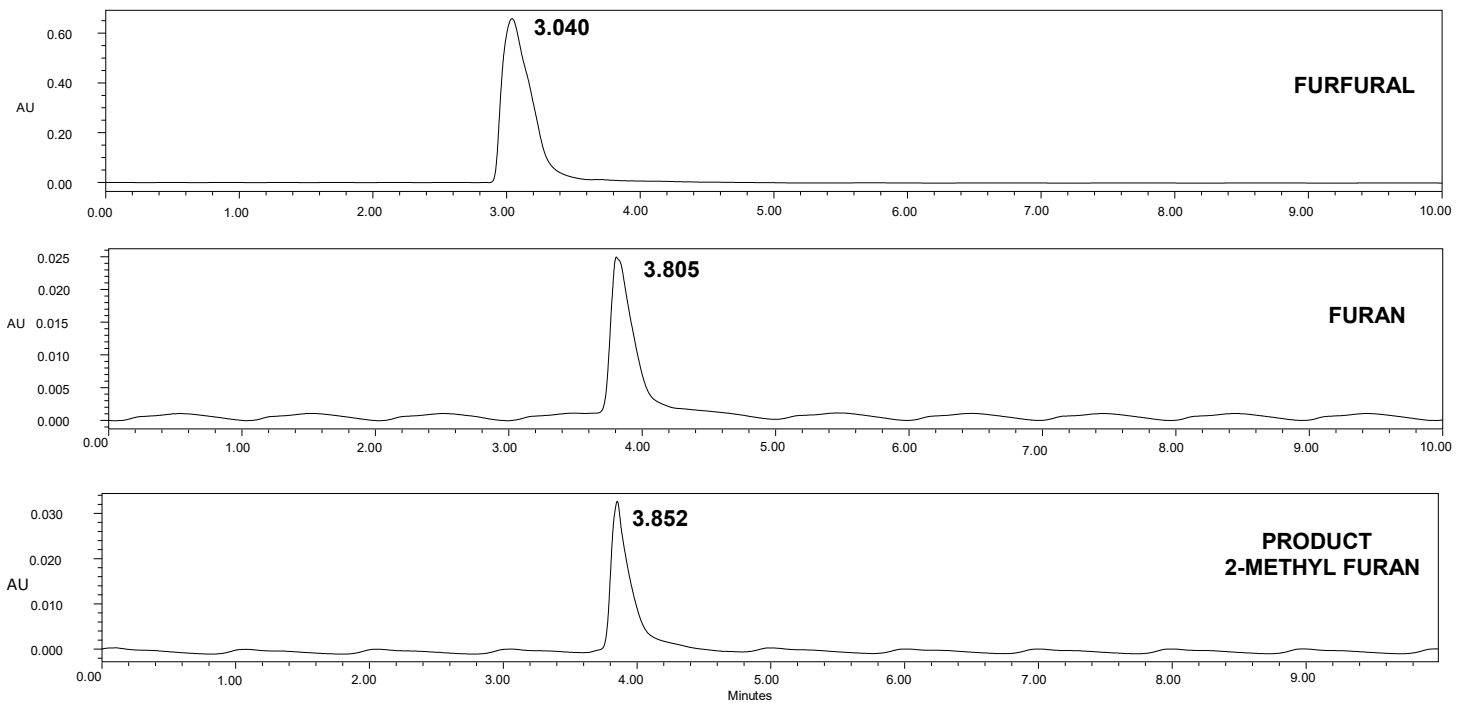


Fig. S15 HPLC chromatogram of reference furfural, furan, and 2-methyl furan product

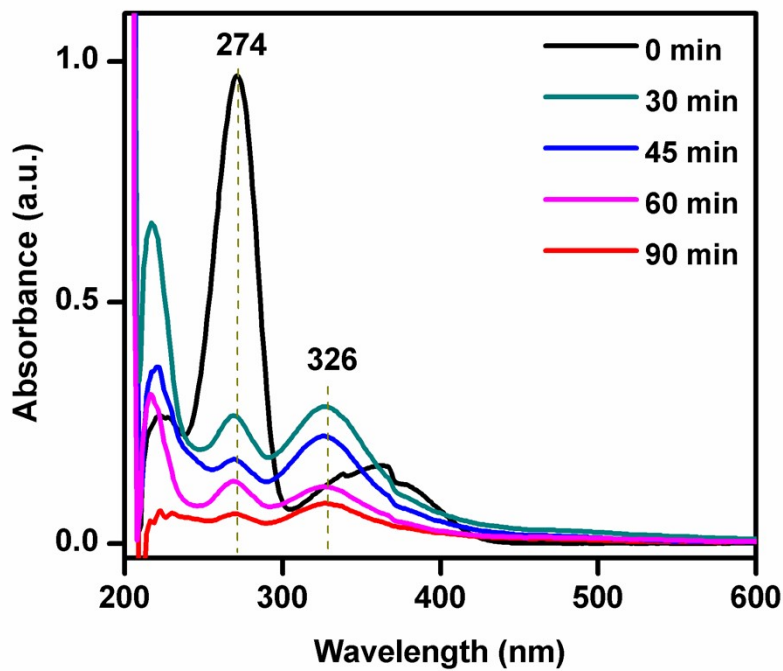


Fig. S16 Time-scaled UV-visible spectra for the catalytic transformation reaction of furfural to 2-MF in the presence of ZnCC@AuNPs and NaOH at 60 °C in IPA.

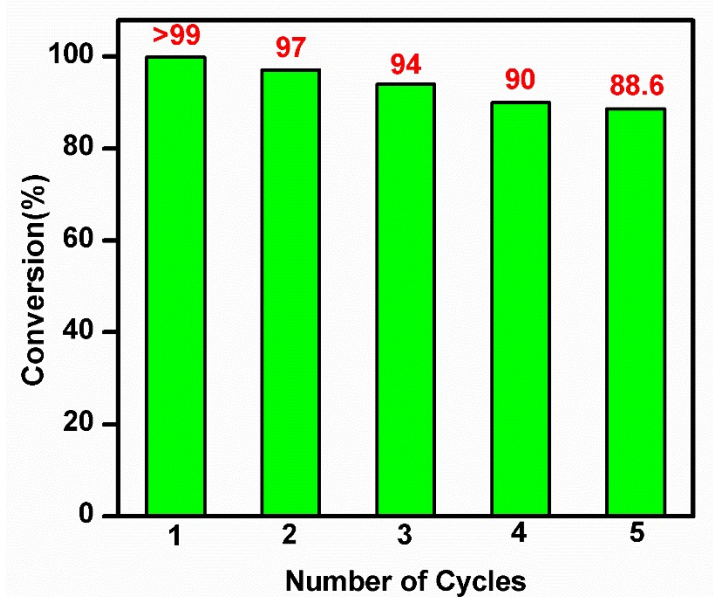


Fig. S17 Recyclability of the ZnCC@AuNPs catalyst

Table S1 Crystallographic data and structural parameters for zinc(II) cubane.

PARAMETERS	VALUE	PARAMETERS	VALUE
Empirical formula	C ₁₀ H ₁₄ BrNO ₃ Zn	μ/mm ⁻¹	4.409
Formula weight	341.50	F(000)	2720.0
Temperature/K	231(100)	Crystal size/mm ³	0.12 × 0.12 × 0.08
Crystal system	Tetragonal	Radiation	Mo Kα ($\lambda = 0.71073$)
Space group	I4 ₁ /a	2Θ range for data collection/°	6.526 to 54.596
a/Å	21.6092(4)	Index ranges	-27 ≤ h ≤ 26, -24 ≤ k ≤ 27, -15 ≤ l ≤ 15
b/Å	21.6092(4)	Reflections collected	23513
c/Å	12.5140(4)	Independent reflections	3100 [R _{int} = 0.0564, R _{sigma} = 0.0448]
α/°	90	Data/restraints/parameter	3100/0/147
β/°	90	Goodness-of-fit on F ²	1.028
γ/°	90	Final R indexes [I>=2σ (I)]	R ₁ = 0.0360, wR ₂ = 0.0674
Volume/Å ³	5843.5(3)	Final R indexes [all data]	R ₁ = 0.0545, wR ₂ = 0.0713
Z	16	Largest diff. peak/hole / e Å ⁻³	0.47/-0.40
ρ _{calc} g/cm ³	1.553		

Table S2 Bonding parameters for zinc(II) cubane.

Bond angles (°)					
O1Zn1N1	96.14(9)	C7N1C8	112.9(2)	O2C9C8	110.5(2)
O1Zn1O2 ³	103.05(8)	C8N1Zn1	110.12(17)	C4C3C2	119.3(3)
O1Zn1O2 ²	109.26(8)	N1C7C6	111.5(2)	O1C1C6	121.5(3)
N1C8C9	109.8(2)	C5C6C7	119.9(3)	N1Zn1O2	76.24(8)
C7N1Zn1	111.19(19)	C1C6C7	120.3(3)	O1C1C2	120.3(3)
C9O2Zn1 ¹	123.46(17)	O1Zn1O2	171.77(7)	C2C1C6	118.1(3)
O2 ³ Zn1N1	134.48(8)	C9O2Zn1	126.66(17)	C3C4C5	120.4(3)
O2 ³ Zn1O2	80.73(8)	C9O2Zn1	106.91(15)	O2 ² Zn1O2	77.86(7)
C1O1Zn1	118.25(18)	C3C4Br1	119.5(2)	O2 ³ Zn1O2 ²	89.63(8)
C5C4Br1	120.1(2)	C5C6C1	119.7(3)	C4C5C6	120.7(3)
Bond length (Å)					
Zn1-O1	1.965(2)	O1-C1	1.334(3)	C9-C8	1.507(4)
Zn1-N1	2.023(2)	N1-C7	1.478(4)	C9-O2	1.421(3)
Zn1-O2	2.4286(19)	N1-C8	1.479(4)	C3-C4	1.376(4)
Zn1-O2 ³	1.9767(19)	C7-C6	1.513(4)	C3-C2	1.385(4)
Zn1-O2 ¹	1.9980(18)	C6-C1	1.408(4)	C1-C2	1.392(4)
Br1-C4	1.903(3)	C6-C5	1.387(4)	C4-C5	1.378(4)

Table S3 Comparison of the catalytic activity of different catalysts for the conversion of furfural to 2-methyl furan

S.No.	Catalyst	Solvent	Time	Temperature (°C)	Conversion(%)	Yield (%) 2-MF	Ref
1.	CuRe/Al ₂ O ₃	i-PrOH	4h	220	100	94	[22]
2.	Cu _{2.5} Zn-Al-	i-PrOH	4h	180	99	72	[23]
			600				
3.	CuFe ₂ O ₄	i-PrOH	1.5h	200	99.4	97	[24]
4.	Iridium/Carbo	i-PrOH	5h	220	99	95	[25]
	n						
5.	Cu ₁ Re _{0.14}	i-PrOH	6h	200	100	86.4	[26]
6.	Cu/ZnO	-	24h	200	100	94.0	[27]
7.	Cu-Fe	-	14h	220	99.4	51	[28]
8.	Cu-Co/ Al ₂ O ₃	i-PrOH	4h	220	100	78	[29]
9.	ZnCC@AuNP	i-PrOH	1.5h	80	100	98.60	This work